Grainyhead-like 2 regulates epithelial morphogenesis by establishing functional tight junctions through the organization of a molecular network among claudin3, claudin4, and Rab25

Kazunori Senga[a,*], Keith E. Mostov[b], Toshihiro Mitaka[c], Atsushi Miyajima[a], and Naoki Tanimizu[a,b,c,*]
[a]Institute of Molecular and Cellular Biosciences, University of Tokyo, 1-1-1 Yayoi, Bunkyo-ku, Tokyo 113-0032 Japan; [b]Department of Anatomy and Department of Biochemistry and Biophysics, University of California, San Francisco, San Francisco, CA 94143-2140; [c]Department of Tissue Development and Regeneration, Research Institute for Frontier Medicine, Sapporo Medical University School of Medicine, S-1, W-17, Chuo-ku, Sapporo 060-8556, Japan

ABSTRACT **During development, epithelial progenitors establish intercellular junctions, including tight junctions (TJs), and form three-dimensional (3D) tissue structures, which are often associated with luminal structures. Here we identify grainyhead-like 2 (Grhl2) as a transcription factor that regulates the size of luminal space surrounded by polarized epithelial cells. We show that HPPL, a liver progenitor cell line, transfected with Grhl2 cDNA forms remarkably larger cysts than the control cells in 3D cultures. We find that Grhl2 up-regulates claudin (Cldn) 3 and Cldn4, and their functions are necessary for the formation of large cysts. Overexpression of Cldn3 alone induces the cyst expansion. In contrast, expression of Cldn4 alone does not induce expansion, as it is not localized at TJs. Of interest, Rab25, another Grhl2 target, not only increases the Cldn4 protein, but also enhances its localization at TJs. Taken together, the results indicate that Grhl2 regulates epithelial morphogenesis through transcriptional up-regulation of Cldn3 and Cldn4, as well as of Rab25, which increases the Cldn4 protein and its localization at TJs. The results reveal a molecular network regulating epithelial lumen formation organized by Grhl2.**

Monitoring Editor
Asma Nusrat
Emory University

Received: Feb 8, 2012
Revised: Jun 4, 2012
Accepted: Jun 7, 2012

INTRODUCTION

Epithelial cells are polarized and form tissue structures required for epithelial organs to perform their physiological functions. Cultured cells have been used to study molecular mechanisms underlying epithelial polarization and tissue morphogenesis (Bryant and Mostov, 2008; Martin-Belmonte and Mostov, 2008; Gray *et al.*, 2010). However, since cell lines used in those studies, such as Mardin–Darby canine kidney (cells or Caco-2 and MCF7 tumor cells, were mostly generated from adult tissues, the processes and mechanisms by which epithelial progenitor cells establish apicobasal polarity and form tissue structures during organogenesis remained largely unknown.

In the liver, two types of epithelial cells—hepatocytes and cholangiocytes—form hepatic cords and bile ducts, respectively. Bile ducts are tubular structures connecting the liver to the small intestine to drain bile secreted from hepatocytes. Bile ducts are lined by cholangiocytes, which modulate the composition of the bile by secreting water and ions (Fitz, 2002). For proper function of the liver, the bile composition needs to be strictly controlled, and any leakage of cytotoxic bile into the parenchyma must be prevented while the bile flows through the liver tissue. Given those physiological functions, establishment of tight junctions (TJs) that control paracellular efflux of small substances is a critical step during the development of bile ducts. Around embryonic day 15 (E15), hepatoblasts—fetal liver stem cells—differentiate into cholangiocytes near the portal vein and form the ductal plate, a single layer of cholangiocytes, which is subsequently reorganized to form tubular structures (Lemaigre, 2003). At an early stage of the reorganization of the ductal plate, cholangiocytes form TJs recognized by ZO1 expression (Antoniou *et al.*, 2009; Zong *et al.*, 2009). However, it remains

This article was published online ahead of print in MBoC in Press (http://www.molbiolcell.org/cgi/doi/10.1091/mbc.E12-02-0097) on June 13, 2012.

*These authors contributed equally to this work.

Address correspondence to: Naoki Tanimizu (tanimizu@sapmed.ac.jp).

Abbreviations used: 3D, three-dimensional; Cldn, claudin; CPE, *Clostridium perfringens* enterotoxin; Grhl2, grainyhead-like 2; TJ, tight junction.

unknown whether those TJs are functional and how immature cholangiocytes establish mature TJs.

Comparison of gene expression profiles between epithelial cells and their progenitors may be an effective way to identify genes regulating epithelial morphogenesis. In this study, we compared neonatal cholangiocytes, which are undergoing tubular morphogenesis, with hepatoblasts by microarray and identified grainyhead-like 2 (Grhl2) as a transcription factor specifically expressed in cholangiocytes. Furthermore, by studying functions of Grhl2 and its target genes in three-dimensional (3D) culture system of liver progenitor cells, we revealed a novel molecular pathway conferring TJ integrity on epithelial progenitors and regulating epithelial morphogenesis.

RESULTS

Comparison of gene expression profiles between hepatoblasts and cholangiocytes isolated from developing liver

Epithelial cells form 3D tissue structures in many organs. In 3D culture, they form cysts, spherical structures with the central lumen surrounded by the polarized epithelial monolayer (Zegers *et al*., 2003). HPPL, a liver progenitor cell line, can form such cysts in 3D culture (Tanimizu *et al*., 2007). However, we realized that, compared with mature cholangiocytes isolated from adult mouse liver, HPPL formed cysts with much smaller lumens (Figure 1A), suggesting that HPPL may lack a critical factor inducing characteristics of mature epithelial cells, such as the formation of cysts with a large central lumen. Because tubular structures with apical lumen become evident around the portal vein in the late gestation and the neonatal stages, we considered the possibility that genes up-regulated in cholangiocytes in these developmental stages might play a role in the formation and/or maturation of luminal structures. To identify key molecules in the formation and/or maturation of luminal structures of tubular ducts, we isolated hepatoblasts (fetal liver stem cells) and neonatal cholangiocytes based on the expression of Dlk and EpCAM, respectively (Supplemental Figure S1) and performed a microarray analysis to identify genes preferentially expressed in cholangiocytes undergoing tubular morphogenesis (Supplemental Tables S1 and S2).

Grainyhead-like 2 enhances epithelial characteristics of liver progenitor cells

Among those genes up-regulated in cholangiocytes, we focused on transcription factors, ankyrin repeat domain 1 (Ankrd1), ets homologous factor (Ehf), grainyhead-like 2 (Grhl2), hairy/enhancer-of-split related with YRPW motif 1 (Hey1), and scleraxis (Scx) as candidate genes regulating epithelial morphogenesis of cholangiocytes. To find a gene implicated in increasing the lumen size, we overexpressed each transcription factor in HPPL and performed 3D culture. We found that only Grhl2 remarkably increased the lumen size of HPPL cysts (Figure 1, B and C).

Grhl2 is a mammalian homologue of *Drosophila* grainyhead, which is implicated in epithelial morphogenesis (Werth *et al*., 2010; Pyrgaki *et al*., 2011). However, expression of Grhl2 in the liver and its functions during the development of epithelial organs, including the liver, has not been reported. First, we performed quantitative PCR and confirmed the expression of Grhl2 in EpCAM$^+$ cholangiocytes at both P0 and adult stages (Supplemental Figure S2A). We also examined the expression of Grhl1 and Grhl3, the other members of the mammalian grainyhead family, and confirmed that only Grhl2 was expressed in cholangiocytes (Supplemental Figure S2B). Next we immunohistochemically examined the expression of Grhl2 in E17.5, P1, and P8 livers. Grhl2 was detected in the nuclei of EpCAM$^+$ cholangiocytes in P1 and P8 livers (Figure 1D, 4–9), whereas it was not expressed in E17.5 liver, where most cholangiocytes form ductal plates (Figure 1D, 1–3). These results suggested that Grhl2 is not involved in the differentiation of cholangiocytes from bipotential hepatoblasts, but it might regulate a later stage, that is, structural and/or functional maturation of bile ducts.

Grhl2 enlarges the lumen without promoting cell proliferation

Because large cysts derived from HPPL expressing Grhl2 (HPPL-Grhl2) apparently consisted of more cells than those from the control HPPL (Figure 1C), increased proliferation might result in large lumens. Actually, at day 7, the lumens of HPPL-Grhl2 cysts consisted of more cells as compared with the control cysts (Figure 2A). On the other hand, a similar number of cells formed the lumens of the control and HPPL-Grhl2 cysts at day 4 (Figure 2B). We monitored the process of lumen expansion from day 2.5 of 3D culture under a microscope and found that HPPL-Grhl2 rapidly expanded the lumen without changing the number of cells (Figure 2C). Thus it is unlikely that Grhl2-induced expansion of lumen was promoted by cell proliferation.

Grhl2 enhances epithelial barrier by up-regulating the expression of Cldn3 and Cldn4

Epithelial cells establish intercellular junctions, including TJs, during development. Although the correlation between the formation of TJs and epithelial morphogenesis has not been adequately clarified, we considered the possibility that maturation of TJs might be coupled with the expansion of a central lumen of cysts. A major physiological function of TJs is forming the paracellular epithelial barrier. We examined the permeability of dextran through the monolayer, which has been used to verify the formation of the epithelial barrier. The results showed that adult cholangiocytes and HPPL-Grhl2 that formed large cysts established a monolayer with strong barrier function as compared with the control HPPL (Figure 3, A and B). Among components of TJs, claudins (Cldns) regulate paracellular permeability of small substances, including ions, by forming paracellular channels (Tsukita and Furuse, 2002). The microarray data indicated that Cldn2, 3, 4, 6, 7, and 8 might be up-regulated when hepatoblasts differentiate to cholangiocytes (Supplemental Table S3). Therefore we addressed whether those molecules mediate the function of Grhl2. First, we compared the expression of these Cldns in HPPL-Grhl2 with that in the control HPPL and found that mRNA levels of Cldn3, 4, and 8 were slightly increased by Grhl2 (Figure 3C). Of interest, Cldn3 and 4 proteins were clearly increased by Grhl2 (Figure 3D). They were detected in the Triton X-100–soluble fraction and also the insoluble fraction, in which TJ proteins are enriched (Figure 3E). Furthermore, immunocytochemistry revealed that Cldn3 and 4 proteins were colocalized with ZO1 at cell–cell contacts, indicating that both are at TJs in HPPL-Grhl2 (Figure 3, F and G). These results suggested that Grhl2 promoted the barrier function of bile ducts by up-regulating Cldn3 and 4 proteins.

Grhl2 expands the lumen of HPPL cysts via Cldn3 and Cldn4

Next, to examine roles of claudins in lumen formation, we took advantage of 3D culture of HPPL. We examined localization of Cldn3 and 4 in cysts derived from HPPL-Grhl2 and found that they were colocalized with ZO1, indicating their localization at TJs (Figure 4A). Then, we added the C-terminal peptide derived from *Clostridium perfringens* enterotoxin (C-CPE), which has been shown to bind Cldn3, 4, and 6 and inhibit their function (Moriwaki *et al*., 2007). glutathione *S*-transferase (GST)–C-CPE peptide excluded Cldn3 and 4 from TJs (unpublished data). In the presence of the GST-fusion protein of C-CPE peptide, HPPL-Grhl2 formed smaller lumens

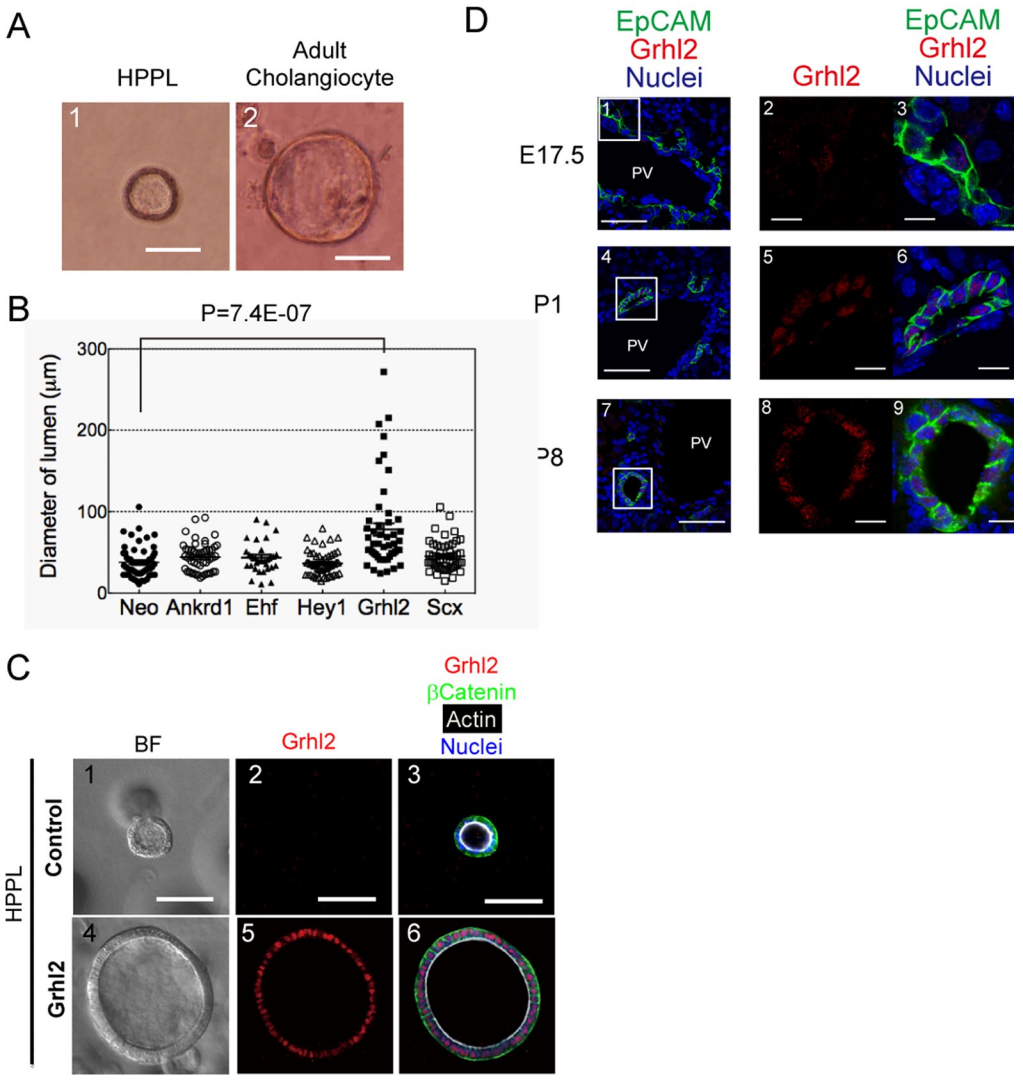

FIGURE 1: Grhl2 enlarges the central lumen of cysts. (A) Mature cholangiocytes form larger cysts than HPPL. Mature cholangiocytes were isolated from mouse adult liver based on the expression of EpCAM. EpCAM$^+$ cholangiocytes and HPPL were cultured in gel containing Matrigel for 7 d. Bar, 50 μm. (B) Effects of transcription factors on the size of a central lumen. HPPL were introduced with retrovirus containing cDNA of Ankrd1, EHF, Hey1, Grhl2, or Scx and used for 3D culture. After 7 d of incubation, pictures were taken for at least 20 areas for measuring the size of cysts. A dot plot with bars of mean ± SEM for a representative culture indicates that the diameter of lumen derived from HPPL expressing Grhl2 (HPPL-Grhl2) is larger than the control with statistical significance. (C) Cyst structures in 3D culture of control HPPL and HPPL-Grhl2. Both HPPL and HPPL-Grhl2 cysts show apical actin bundles (white) and basal β-catenin (green), whereas cysts derived from HPPL-Grhl2 have remarkably larger lumen (4–6) as compared with the control (1–3). The control HPPL and HPPL-Grhl2 were cultured in gel containing Matrigel for 7 d. Cysts were incubated with anti-Grhl2 and anti–β-catenin antibodies, followed by incubation with secondary antibodies and Alexa Fluor 633–conjugated phalloidin. Nuclei were counterstained with Hoechst 34580. BF, bright field. Bars, 50 μm. (D) Immunofluorescence analysis of Grhl2 expression in developing liver. In E17.5 liver (1–3), Grhl2 (red) is not detectable in EpCAM$^+$ cholangiocytes (green), whereas it is expressed in cholangiocytes forming tubular structures in P1 (4–6) and P8 (7–9). Boxes in 1, 4, and 7 are enlarged in 2/3, 5/6, and 8/9, respectively. Bars, 50 μm (1, 4, and 7), 10 μm (2, 3, 5, 6, 8, and 9).

compared with the culture with C-CPE313 peptide, an inactive mutant (Figure 4, B and C). Thus functions of Cldns were indispensable for the Grhl2-induced enlargement of cysts.

We also overexpressed Cldn3 or Cldn4 in HPPL (Supplemental Figures S3 and S4). As shown in Figure 4, D and E, Cldn3 alone, but not Cldn4, increased the size of lumen. Moreover, cysts derived from HPPL-Cldn3+4 formed lumens similar in size to those derived from HPPL-Cldn3 (Supplemental Figure S5). We found that Cldn4 was not localized at TJs in HPPL-Cldn4 (see later discussion of Figure 6), which provides a possible explanation for why expression of Cldn4 alone did not increase the size of lumen. On the other hand, Cldn4 was localized at TJs in HPPL-Grhl2 (Figure 4A, 13–16), suggesting that an additional factor induced by Grhl2 may be necessary for Cldn4 to be localized at TJs and thereby be functional (see later discussion).

Grhl2 enlarges the central lumen of cysts by up-regulating Rab25

Because the expression of Cldn3 and 4 was not sufficient to mimic the effect of Grhl2 on lumen size, other targets of Grhl2 were likely to be involved. The consensus DNA sequence for Grhl2 binding was

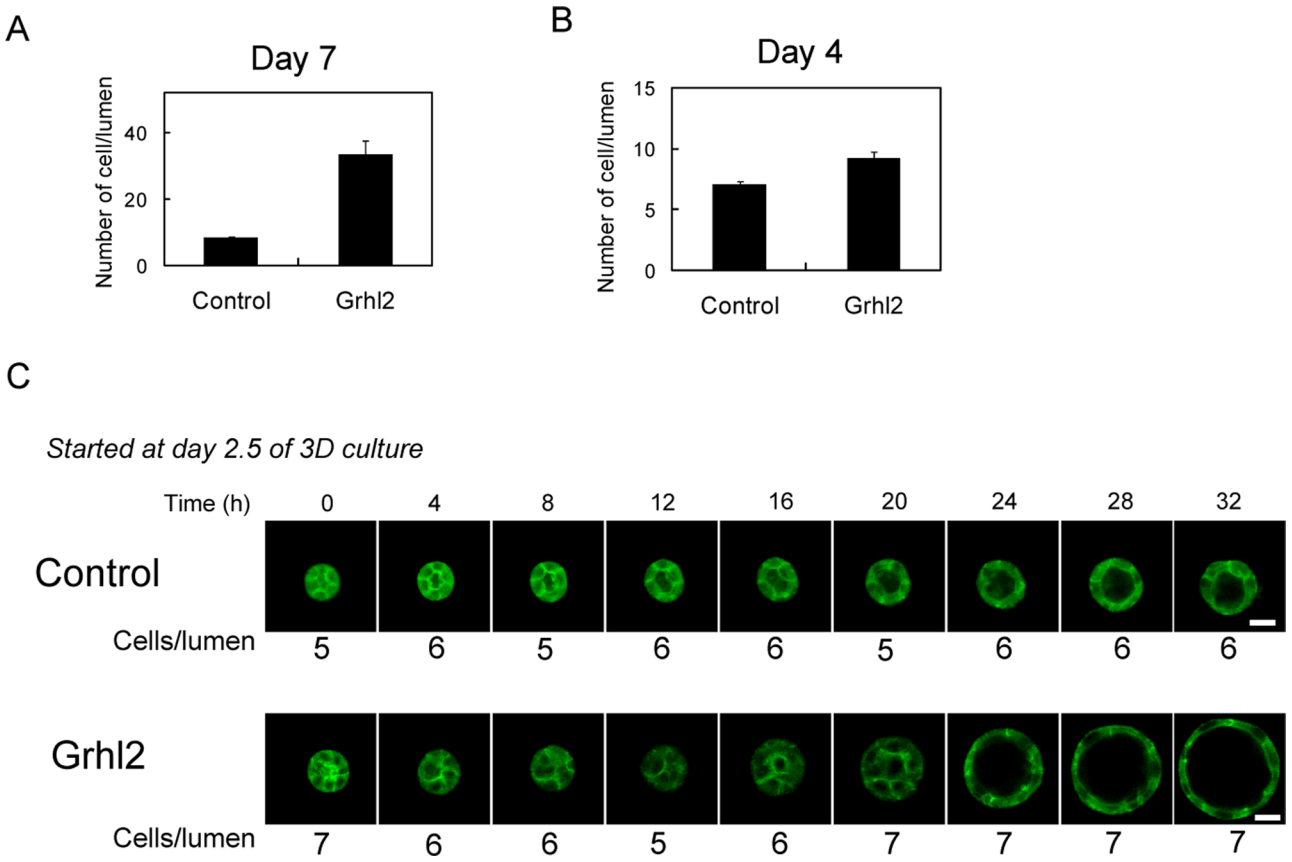

FIGURE 2: HPPL-Grhl2 starts expanding the lumen without proliferation. (A) Cysts derived from HPPL-Grhl2 contain more cells than the control at day 7 of 3D culture. Cysts were fixed in 4% PFA, and nuclei were stained with Hoechst 34580. Pictures were taken on a microscope, and the number of cells surrounding the lumen was counted. (B) Cysts derived from HPPL-Grhl2 contain similar number of cells at day 4 of 3D culture. (C) HPPL-Grhl2 expands the lumen without changing the number of cells forming the lumen. Images of cysts derived from the control HPPL and HPPL-Grhl2 at different time points were taken under a confocal microscope. The numbers of cells around the lumen are indicated under the image at each time point. Bars, 50 μm.

reported as AACCGGTT (Werth *et al.*, 2010). Using a database of mouse and human genomes, we searched for genes that have this sequence in the proximal promoter (within 1000 base pairs from the transcription initiation site) in both mice and humans. Furthermore, we analyzed whether candidate genes were up-regulated in neonatal cholangiocytes as compared with hepatoblasts in the microarray data to find Grhl2 targets important for the enlargement of lumen (Supplemental Table S4). As a result, we identified several genes, including the small GTPase Rab25, as possible targets of Grhl2 (Figure 5A). We further confirmed that Rab25 was specifically up-regulated in the cholangiocyte lineage during in vivo bile duct development, and it was significantly increased by overexpression of Grhl2 (Supplemental Figure S6). There is one putative binding site for Grhl2 (Grhl2-binding element; GBE in Figure 5B) and one similar sequence (GBE? in Figure 5B) within 150 base pairs upstream of the transcription site. Promoter reporter assays using deletion mutants of the promoter region revealed that the putative binding site was necessary for Grhl2 to promote transcription (Figure 5B). These data strongly suggested that Rab25 is a target of Grhl2.

Next we established HPPL-Rab25, and their 3D culture showed that Rab25 increased lumen size (Figure 5, C and D). In contrast, a dominant-negative form of Rab25 partially inhibited the expansion of a central lumen induced by Grhl2 (Figure 5, E and F). These results suggested that Grhl2 regulated epithelial morphogenesis of HPPL through Rab25.

Rab25 increases Cldn4 protein and regulates its localization at TJs

We considered the possibility that Rab25 might regulate the expression and intracellular localization of Cldn4. Indeed, we found that Rab25 overexpression resulted in an increase of Cldn4 protein (Figure 6A), although it did not increase Cldn3 protein. Because Rab25 limited paracellular permeability of 4-kDa fluorescein isothiocyanate (FITC)–dextran (Figure 6B), Cldn4 in HPPL-Rab25 might be functional at TJs. We further performed immunofluorescence analysis and found colocalization of Cldn4 and ZO1 in cysts formed from HPPL-Rab25 (Figure 6C). Quantitative analysis confirmed that Rab25 induced colocalization of Cldn4 and ZO1 (Figure 6D and Supplemental Figure S7). By contrast, Cldn4 was mostly localized at the basolateral domain in HPPL-Cldn4. Consistently, dominant-negative Rab25 abolished colocalization of Cldn4 and ZO1 (Figure 6, E and F). These data indicated that Rab25 regulates the barrier function and morphogenesis of liver progenitor cells by up-regulating Cldn4 at TJs.

Molecular link among Cldn3, Cldn4, and Rab25

Grhl2 enhances the epithelial characteristics of HPPL through Cldn3, Cldn4, and Rab25. However, it was not clear how much the Grhl2 functions depend on these three molecules. Although Grhl2 up-regulates Cldn4 at the transcriptional level, the data in Figure 5 suggested that Cldn4 functions in HPPL depend on Rab25. Therefore we introduced both Cldn3 and Rab25 to HPPL (HPPL-Cldn3+Rab25)

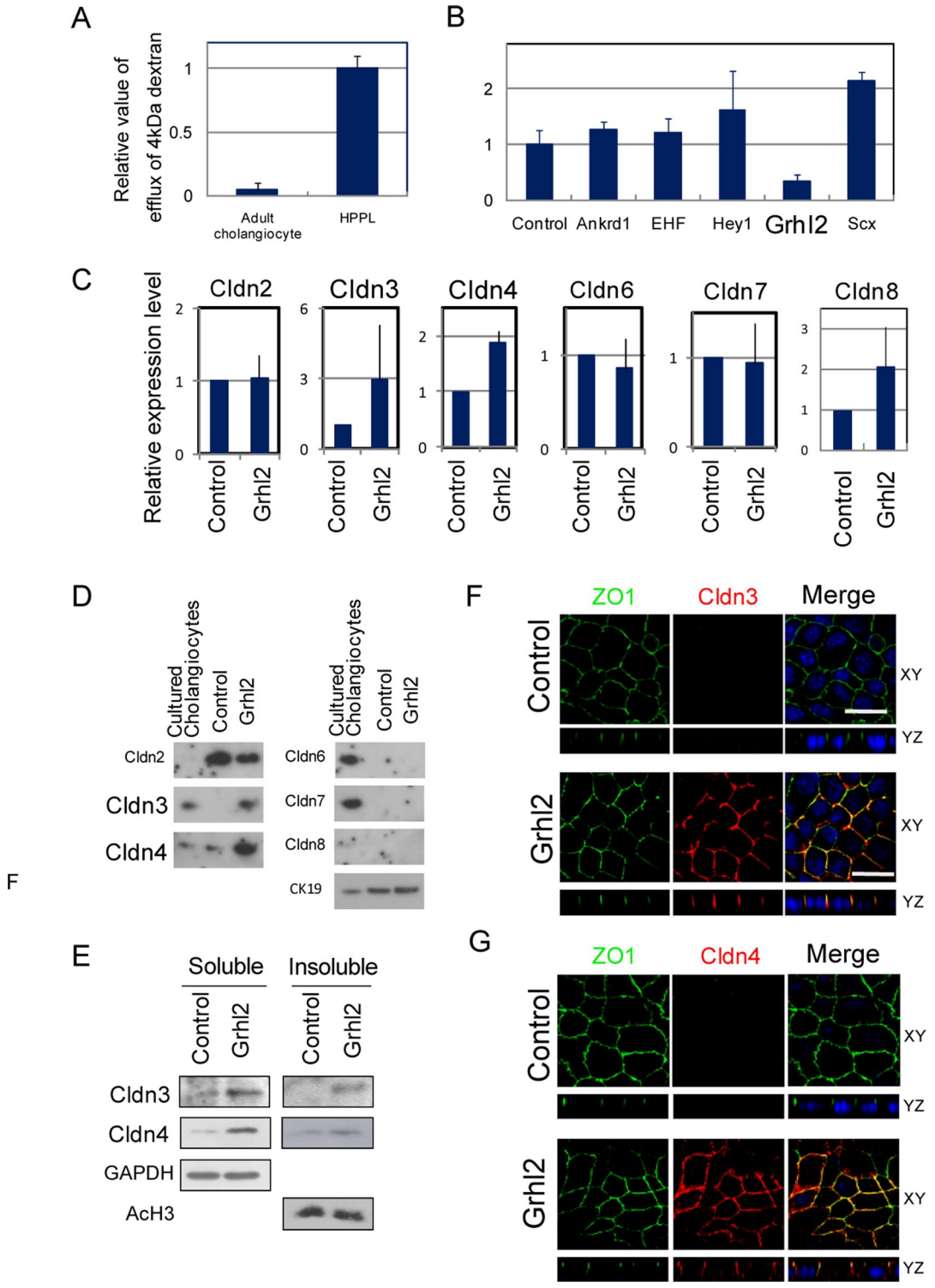

FIGURE 3: Grhl2 increases epithelial barrier function of HPPL by up-regulating Cldn3 and 4. (A) Adult mature cholangiocytes show stronger barrier functions than HPPL. Adult cholangiocytes were isolated as EpCAM$^+$ cells and plated onto a culture insert coated with type I collagen gel. HPPL were plated on a culture insert coated with laminin. FITC-dextran, 4 kDa, 1 mg/ml was added inside the culture insert, and 2 h later the medium in the bottom was used for measuring the fluorescence of FITC. (B) Grhl2 decreases the efflux of 4-kDa FITC-dextran through the monolayer of HPPL. (C) PCR analysis for expression of Cldn2, 3, 4, 6, 7, and 8. Cldn3, 4, and 8 are transcriptionally up-regulated by overexpression of Grhl2. (D) Western blot analysis for expression of Cldn2, 3, 4, 6, 7, and 8. Grhl2 increases Cldn3 and 4 proteins as compared with the control. (E) Detection of Cldn3 and 4 in Triton X-100–soluble and –insoluble fractions. Grhl2 increases Cldn3 and 4 proteins both in Triton X-100–insoluble fraction, which represents Cldns incorporated into TJs, and in soluble fraction. (F, G) Localization of Cldn3 and 4 in 2D culture. Cldn3 and 4 (red) are colocalized with ZO1 (green), suggesting that they are incorporated into TJs in HPPL-Grhl2. The monolayer of HPPL was stained with anti-ZO1 and either anti-Cldn3 or 4 antibody.

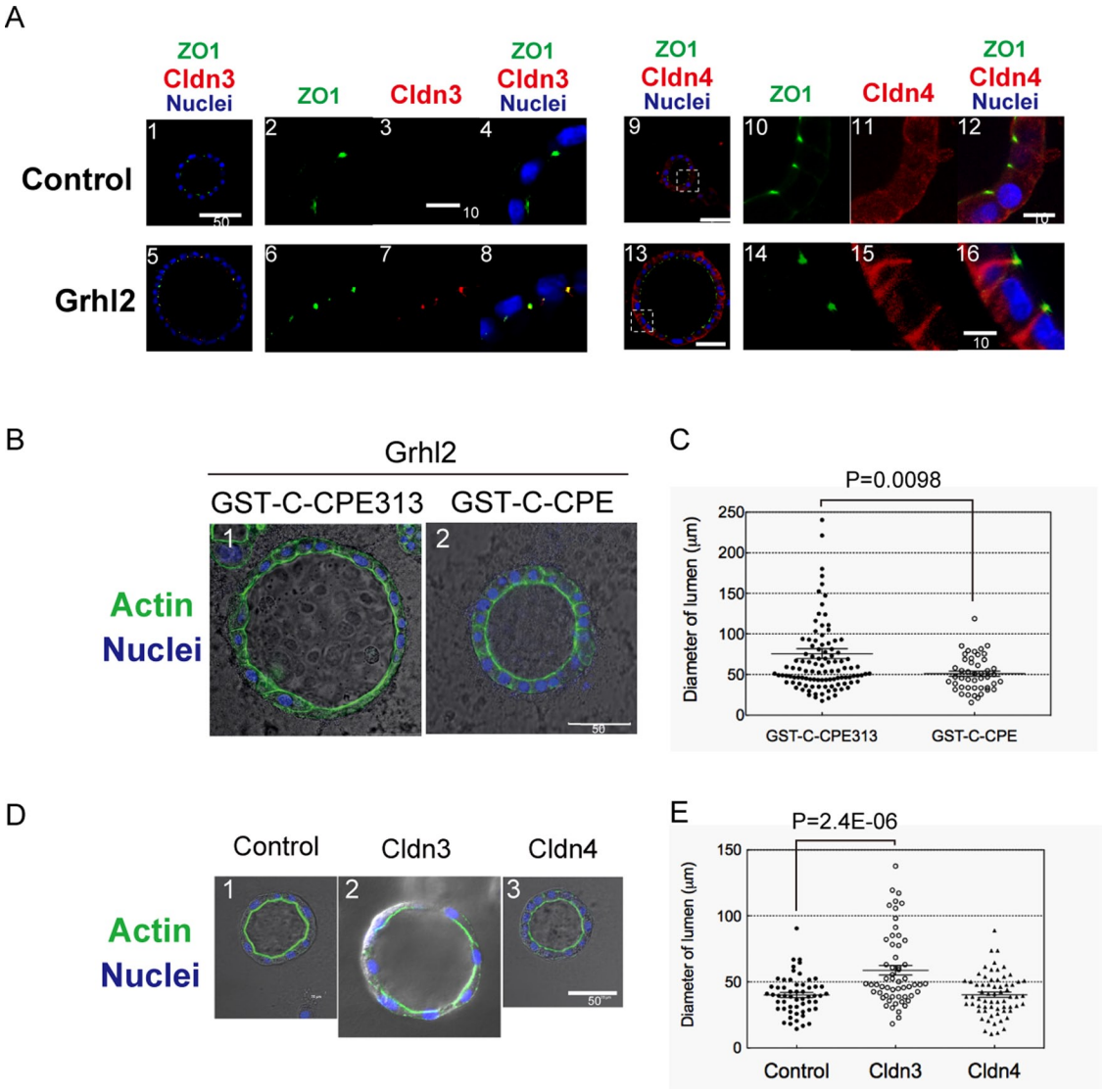

FIGURE 4: Cldn3 and 4 mediate the function of Grhl2 to enlarge a central lumen. (A) Cldn3 and 4 in HPPL-Grhl2 are localized at TJs. Cldn3 (red) expressed in HPPL-Grhl2 is colocalized with ZO1 (green; 5–8). Cldn4 (red) expressed in HPPL-Grhl2 is colocalized with ZO1 (green) in addition to relatively strong expression at the basolateral membrane (13–16). Cysts derived from HPPL and HPPL-Grhl2 were stained with anti-ZO1 and anti-Cldn3 or 4 antibodies. Nuclei were counterstained with Hoechst 34580 (blue). (B, C) Inhibition of Cldns by the C-terminal peptide derived from C-CPE decreases the size of a central lumen. Pictures for representative cysts are shown in B. The central lumen of cysts in the presence of CPE peptide is normally surrounded by F-actin bundle (green) but is remarkably smaller compared with the control. (C) Dot plot with bars of mean ± SEM for a representative culture, indicating that the lumen becomes smaller in the presence of CPE peptide with statistical significance. HPPL and HPPL-Grhl2 were cultured in the presence of 100 μg/ml GST-C-CPE or GST-C-CPE313 (a deletion mutant of C-CPE lacking the capability to bind to Cldns). The diameter of lumen was measured for >50 cysts per culture. Experiment was repeated four times independently. (D, E) Overexpression of Cldn3, but not Cldn4, induces the enlargement of a central lumen. (D) Representative pictures of cysts derived from HPPL, HPPL-Cldn3, and HPPL-Cldn4. Cldn3, but not Clnd4, enlarged the central lumen of a cyst. (E) Dot plot with bars of mean ± SEM for a representative culture, indicating that Cldn3 increases the size of lumen with statistical significance. HPPL, HPPL-Cldn3, and HPPL-Cldn4 were cultured under 3D conditions for 7 d. The diameter of lumen was measured for >50 cysts per culture. Experiment was repeated four times independently.

and examined the effect on epithelial properties of HPPL by comparing with HPPL-Cldn3 and HPPL-Rab25. HPPL-Cldn3+Rab25 significantly increased barrier function, as shown by the decrease in permeability of 4-kDa FITC-dextran (Figure 7A). In addition, in 3D culture, HPPL-Cldn3+Rab25 further increased the size of the central lumen (Figure 7C). The barrier function of HPPL-Cldn3+Rab25 was almost identical to that of HPPL-Grhl2 (Figure 7B). Thus Cldn3, Cldn4, and Rab25 are assumed to mediate the function of Grhl2 to regulate barrier functions of HPPL. However, as cysts derived from HPPL-Cldn3+Rab25 were still slightly smaller than those from HPPL-Grhl2 (Figure 7D), it remains possible that an additional Grhl2 target might be involved in enlargement of the central lumen of cysts.

DISCUSSION

Many epithelial tissues contain a luminal space. Paucity of lumen formation results in abnormal organ development, whereas

uncontrolled expansion of luminal space is observed in polycystic diseases. Thus it is important to regulate the size of lumen. However, in contrast to the initiation of lumen formation, molecular mechanisms regulating the size of lumen remain largely unknown. In this study, we compared neonatal cholangiocytes with hepatoblasts by microarray and identified genes specifically up-regulated in cholangiocytes. Among those genes, we found that a transcription factor, Grhl2, expands the apical luminal space of cysts derived from liver progenitor cells through up-regulation of Cldn3, Cldn4, and Rab25. Because Cldn3 and Cldn4, whose localization at TJs is regulated by Rab25, induce the maturation of TJs, our results linked the establishment of epithelial junctional complexes with the promotion of morphogenesis, in particular, lumen formation.

Grhl2 is a member of the grainyhead transcription factor family, mammalian homologues of *Drosophila* grainyhead. The mammalian grainyhead family consists of three members—Grhl1, 2, and 3. It has been demonstrated that Grhl1 regulates hair anchorage and epidermal differentiation (Wilanowski *et al.*, 2008), whereas Grhl3 regulates skin permeability by modulating the barrier function of epidermis, urothelial differentiation, and dorsal closure of the neural tube (Yu *et al.*, 2008, 2009). Recently Grhl2 was shown to be a key transcription factor completing neural tube closure (Pyrgaki *et al.*, 2011; Werth *et al.*, 2010) and modulating the nature of cell–cell contacts by promoting the formation of the apical junctional complex (Werth *et al.*, 2010). On the other hand, since mice lacking Grhl2 die around E13.5 before the development of most epithelial organs, including the liver, the roles of Grhl2 in epithelial morphogenesis remain unknown. Our data indicating that Grhl2 enhances epithelial barrier function and morphogenesis of liver progenitor cells in vitro show the possibility that Grhl2 regulates structural and functional differentiation of epithelial tissues.

TJs contain Cldns, as well as occludin and junctional adhesion molecules. Among those TJ proteins, Cldns regulate the paracellular transport of small substances (Tsukita and Furuse, 2002). Our results indicate that Grhl2 regulates barrier function of bile ducts by up-regulating Cldn3 and 4. Ectopic expression of Cldn3 resulted in the localization of Cldn3 at TJs and the modest expansion of the central lumen. On the other hand, the introduction of Cldn4 alone did not affect the size of lumens, probably because most of Cldn4 was localized at the basolateral domain (Figure 6, C and D). Although it was previously reported that ectopic expression of Cldn4 resulted in its localization at TJs and increased epithelial barrier, epithelial progenitors such as HPPL might lack a transport system required for the proper localization of Cldn4. Our results show that the Grhl2-Rab25 axis plays a key role in barrier function by localizing Cldn4 at TJs.

Rab25 is a member of the Rab11 subfamily consisting of Rab11a, 11b, and 25. Rab11a and Rab25 are implicated in recycling of apical proteins (Casanova *et al.*, 1999). Rab25 is known to be relatively abundant in gastrointestinal tissues (Goldenring *et al.*, 1993). Recently it was reported that Rab11a and 25 are involved in the formation of apical lumens (Bryant *et al.*, 2010). Because HPPL can form small cysts without Rab25 in 3D culture, it may be dispensable for HPPL to form the apical lumen in our system. On the other hand, Rab25 contributes to the formation of mature epithelial structures by localizing Cldn4 at TJs. Given that Rab25-knockout mice did not show any defects in liver (Nam *et al.*, 2010), Rab11a and Rab25 may have a redundant function in the bile duct development. However, it might be worth examining whether bile ducts without Rab25 are more susceptible to any type of liver injury.

It remains unclear how the Grhl2-Rab25 axis up-regulates Cldn4 and promotes its localization at TJs. Given that Rab25 has been implicated in recycling of apical proteins, it may promote the transport of internalized Cldn4 protein back to TJs, leading to prevention of the traffic of Cldn4 to lysosomes for degradation. Furthermore, a recent article demonstrated that Rab25 but not Rab11a regulates the transcytosis of FcRn from the basolateral to the apical and vice versa (Tzaban *et al.*, 2009). Given that most of Cldn4 is localized at the basolateral domain, Rab25 might be involved in trafficking Cldn4 from the basolateral domain to TJs by transcytosis, possibly through indirect interactions between Rab25 and Cldn4 (Supplemental Figure S8).

We summarize a molecular network governed by Grhl2 in Figure 8. Grhl2 enhances epithelial barrier by up-regulating Cldn3 and Cldn4, which leads to lumen expansion. In addition, Grhl2 enhances lumen expansion by up-regulating Rab25, which up-regulates Cldn4 protein and also regulates its localization at TJs. Strong barrier function is probably a physiological requirement for bile duct tubules to prevent any leakage of cytotoxic bile into the liver parenchyma. In fact, it was recently shown in zebrafish that Cldn15 and Cldn15-like b were necessary for normal formation of intestine (Bagnat *et al.*, 2007) and bile ducts (Cheung *et al.*, 2011), respectively. Our results reveal a novel mechanism regulating the process by which epithelial cells acquire mature epithelial structures necessary for their physiological functions.

MATERIALS AND METHODS

Extracellular matrix, growth factors, and chemicals

Type I collagen was purchased from Koken (Tokyo, Japan). Growth factor–reduced Matrigel and purified laminin-1 were from BD Biosciences (Bedford, MA).

Cell preparation and RNA isolation

Liver cells were isolated from E14.5, E17.5, and P0 livers according to a previous report, with slight modification. Livers were minced and then digested in Librase 3 blenzyme (Roche Applied Science, Indianapolis, IN) that was 50 times diluted in phosphate-buffered saline (PBS) ++. Cells were incubated with anti-mouse EpCAM (BD Biosciences) conjugated with Alexa Flour 488 or FITC-conjugated anti-mouse EpCAM (Okabe *et al.*, 2009). $EpCAM^+$ cells were isolated with a FACSAria. Dlk^+ cells were isolated from E14.5 liver as previously reported (Tanimizu *et al.*, 2003).

Total RNA was isolated from purified Dlk^+ and $EpCAM^+$ cells by using a Purelink RNA mini kit (Ambion, Austin, TX). RNA concentration was measured on a NanoDrop (Thermo Fisher Scientific, Waltham, MA). After checking concentration, we checked the quality of RNA samples on a bioanalyzer (Agilent Technologies, Santa Clara, CA).

Microarray analysis

For comparing hepatoblasts and cholangiocytes, synthesis and labeling of cRNA were performed at the University of California, San Francisco, Sandler Center. Agilent whole genome mouse array (014868) was used for gene expression analysis.

Plasmids

cDNA of Grhl2 was amplified from Kazusa cDNA clone (kindly provided by Osamu Obara, Kazusa DNA Research Institute, Chiba, Japan). cDNAs of Ankrd1, Ehf1, Hey1, Scx, Cldn3, Cldn4, and Rab25 were amplified from first-strand cDNA synthesized from neonatal cholangiocytes or kidney. A dominant-negative form of Rab25 (dn-Rab25) was generated by adding a point mutation in its GTP-binding domain to change Thr26 to Gln (Casanova *et al.*, 1999). After performance of DNA sequencing, they were transferred to a retrovirus vector, pMXsNeo. Infected HPPL were treated with 0.1 mg/ml G418 to select cells introduced with the vector. After the selection, most of the cells expressed transgenes. To express Cldn3 in HPPL-Rab25 and HPPL-Cldn4 or dnRab25 in HPPL-Grhl2, we inserted

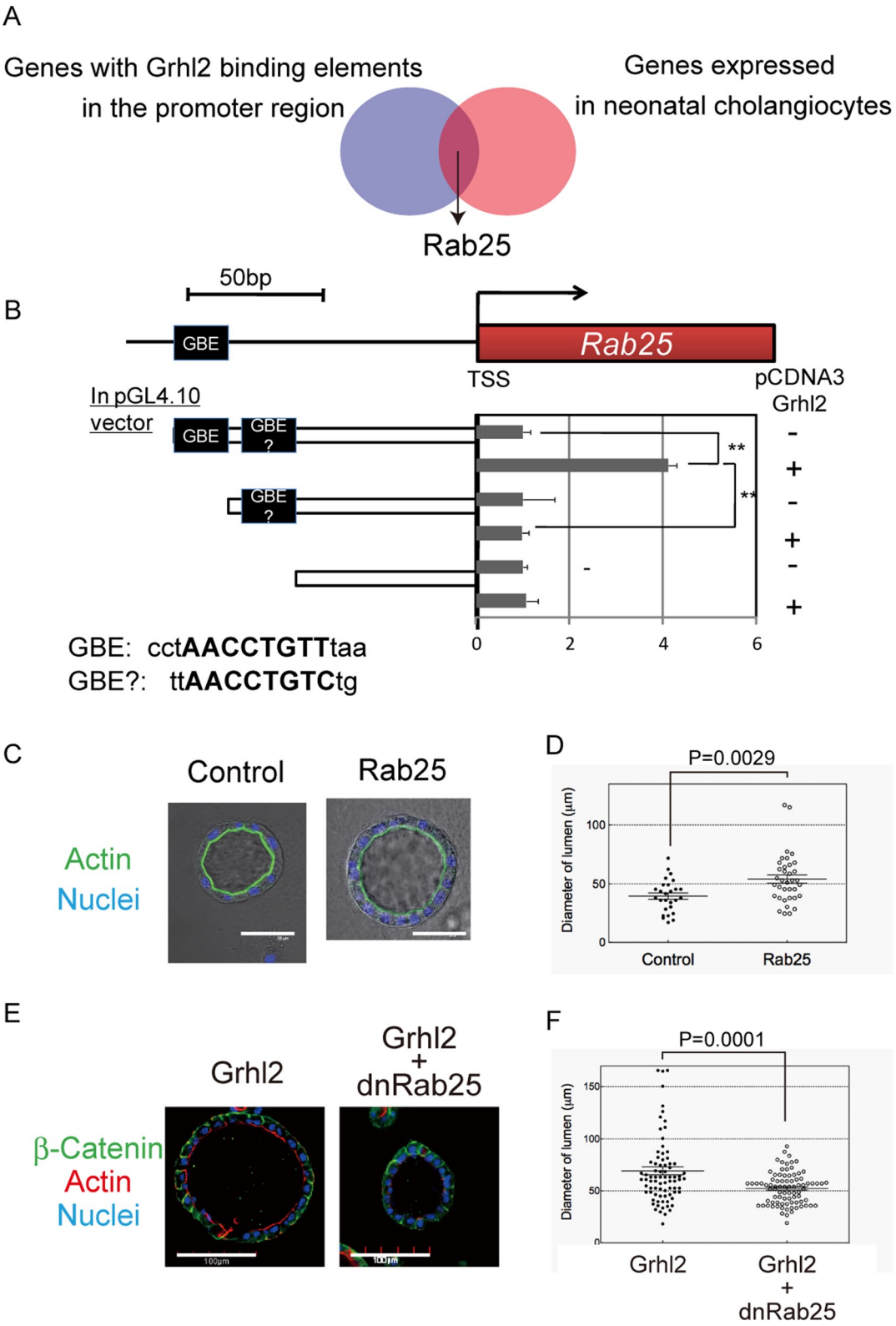

FIGURE 5: The small GTPase Rab25, a target of Grhl2, is involved in the enlargement of a central lumen induced by Grhl2. (A) A schematic view for the identification of Rab25. The consensus DNA sequence for Grhl2 binding (AACCGGTT) was searched in the database for human and mouse genes. More than 1000 genes were found to contain the sequence within 1000 base pairs upstream of the transcription initiation site. Among those genes, Rab25 was selected as a Grhl2 target since it was up-regulated in P1 cholangiocytes (shown by the microarray result comparing neonatal cholangiocytes with hepatoblasts) and might be involved in the intracellular localization of Cldn4. (B) A potential Grhl2-binding site in the promoter region of Rab25 gene is necessary for up-regulation of Rab25 mRNA by Grhl2. Luciferase activity is detected in the presence of Grhl2, whereas the deletion of a possible binding site (GBE) diminishes the expression of luciferase. GBE, grhl2-binding element. (C, D) Overexpression of Rab25 induces the enlargement of a

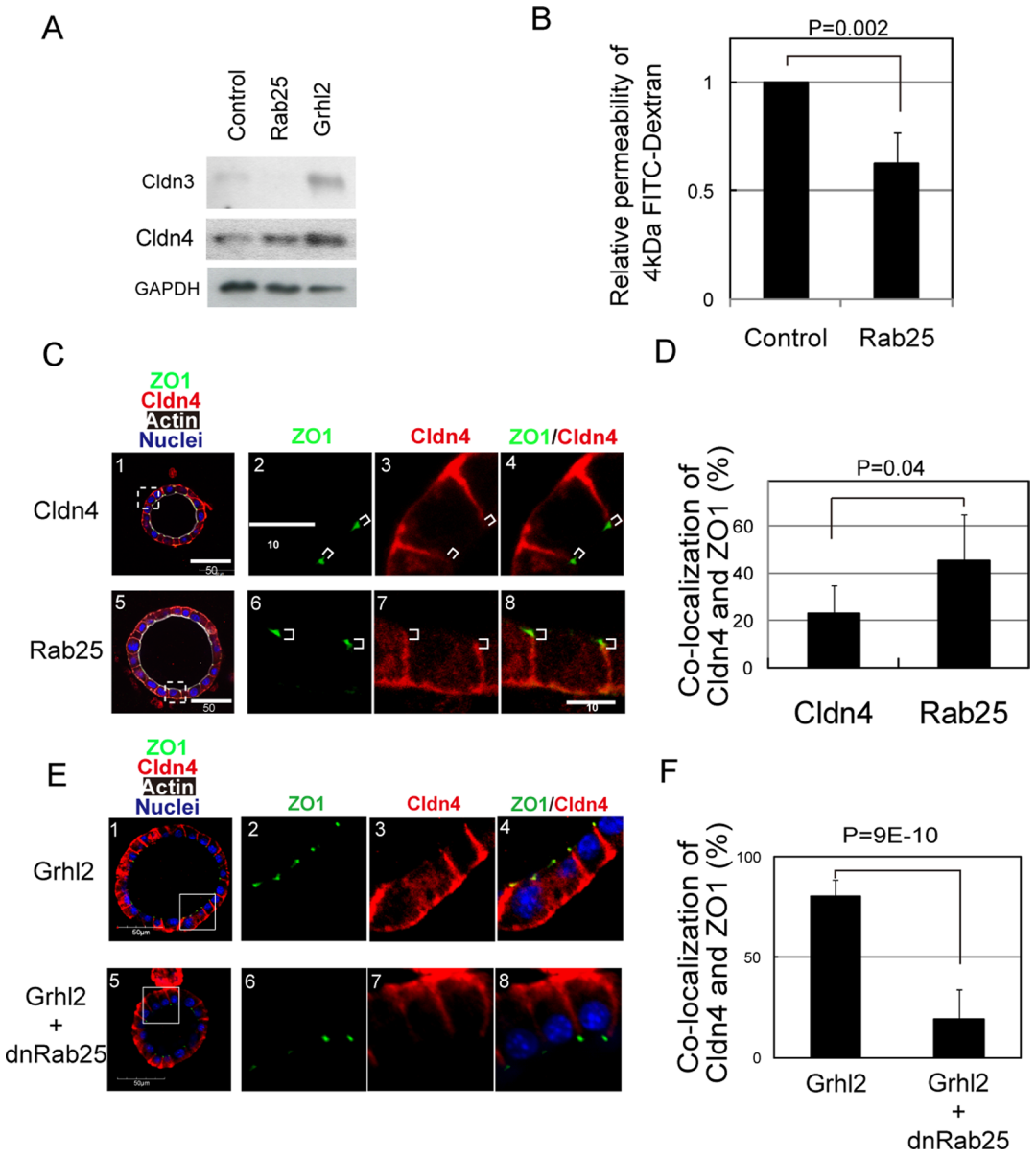

FIGURE 6: Rab25 increases Cldn4 protein and regulates its localization at TJs. (A) Rab25 increases the level of Cldn4 protein. Western blot data demonstrate that Rab25 increases Cldn4 protein but not Cldn3. (B) Rab25 enhances barrier function of the monolayer of HPPL. Rab25 decreases paracellular efflux of 4-kDa FITC-dextran, indicating that the barrier function of HPPL monolayer is enhanced. The control HPPL and HPPL-Rab25 were cultured on Transwells and used to examined the efflux of FITC-dextran. Experiment was repeated three times independently. (C, D) Rab25 promotes the localization of Cldn4 at TJs. Cldn4 (red) is barely colocalized with ZO1 (green) in HPPL-Cldn4 (C1–C4), whereas it is colocalized with ZO1 in HPPL-Rab25 (C5–C8). More than 50 lateral membranes derived from five cysts were analyzed for localization of Cldn4 and ZO1. The result is shown in D, indicating that Rab25 significantly increases colocalization of Cldn4 and ZO1. (E, F) dnRab25 inhibits the localization of Cldn4 at TJs. Cldn4 (red) is colocalized with ZO1 (green) in HPPL-Grhl2 (E1–E4), whereas it is not colocalized with ZO1 in HPPL-Grhl2+Rab25 (E5–E8). More than 100 lateral membranes derived from 10 cysts were analyzed for localization of Cldn4 and ZO1. The result is shown in F, indicating that dnRab25 significantly inhibits colocalization of Cldn4 and ZO1.

central lumen. (C) Representative cysts derived from HPPL and HPPL-Rab25. A cyst derived from HPPL-Rab25 has a central lumen surrounded by F-actin bundles (green) larger than the control HPPL. (D) Dot plot with bars of mean ± SEM for a representative culture, indicating that HPPL-Rab25 increased the size of lumen with statistical significance. HPPL and HPPL-Rab25 were cultured for 7 d, and the diameter of the central lumen was measured for >50 cysts per culture. Experiments were repeated four times independently. Bar, 50 μm. (E, F) Inhibition of Rab25 by a dominant-negative form of Rab25 in HPPL-Grhl2 resulted in decreased lumen size. (E) Representative cysts derived from HPPL-Grhl2 and HPPL-Grhl2+Rab25. Cysts derived from HPPL-Grhl2+dnRab25 have a central lumen smaller than HPPL-Grhl2. (F) Dot plot with bars of mean ± SEM for a representative culture, indicating that dnRab25 reduces the size of the central lumen with statistical significance. HPPL-Grhl2 and HPPL-Grhl2+dnRab25 were cultured for 7 d. The diameter of the lumen was measured >50 cysts per culture. Experiments were repeated for four times independently. Bars, 100 μm.

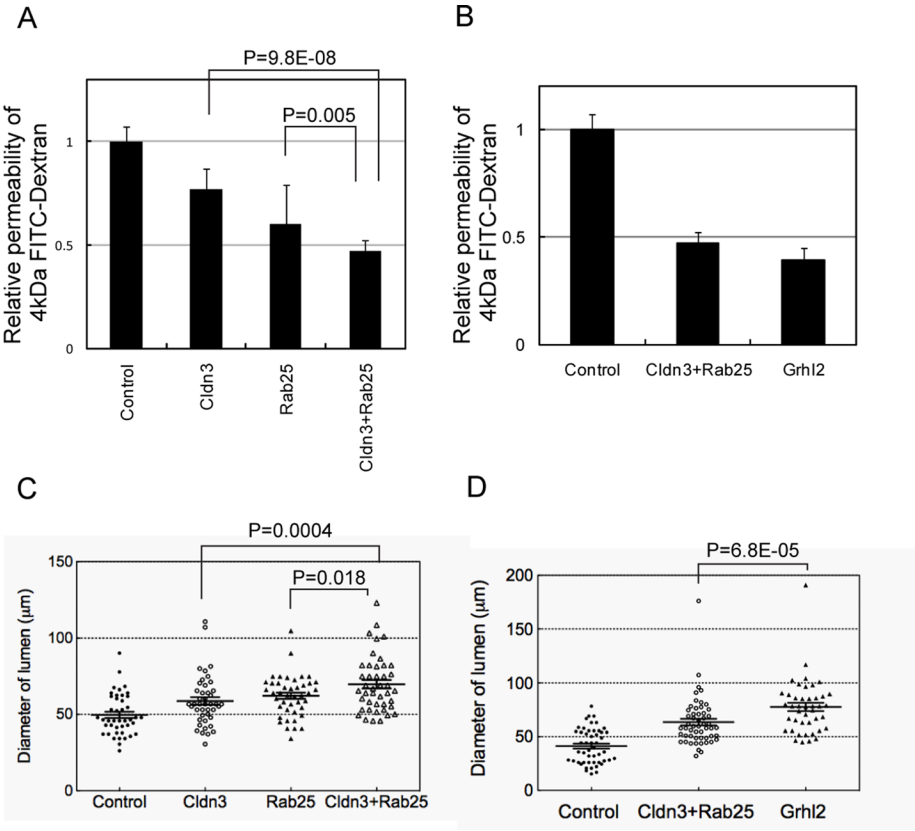

FIGURE 7: Cldn3 and Rab25 have additive effect on increasing barrier function and the lumen size. (A) HPPL-Cldn3+Rab25 shows stronger barrier function than HPPL-Cldn3 or HPPL-Rab25. Paracellular efflux of 4-kDa FITC-dextran is further decreased by coexpression of Cldn3 and Rab25 in HPPL as compared with expression of either of them. (B) HPPL-Cldn3+Rab25 and HPPL-Grhl2 show similar barrier function. (C) HPPL-Cldn3+Rab25 form significantly larger cysts than HPPL-Cldn3 or HPPL-Rab25. The size of lumen is further increased by coexpression of Cldn3 and Rab25 in HPPL as compared with expression of either of them. A dot plot for a representative culture is shown. The diameter of the lumen was measured for >50 cysts per culture. Experiment was repeated for three times independently. (D) HPPL-Grhl2 forms significantly larger cysts than HPPL-Cldn3+Rab25.

Cldn3 or dnRab25 cDNA into another retrovirus vector, pMXsPuro. After infection, HPPL were treated with 10 μg/ml puromycin. The promoter sequence of Rab25 containing 1000 base pairs upstream of the transcription initiation site was amplified from genomic DNA of embryonic kidney. It was inserted into pMD20. The proximal region was amplified and inserted into pGL4 vector.

Immunofluorescence chemistry

Fetal, neonatal, and adult livers were fixed in PBS containing 4% paraformaldehyde (PFA) and embedded in OCT compound. Thin sections were prepared with a microtome. For staining of Cldns in 2D culture of HPPL, samples were fixed in 1% PFA, permeabilized with 0.2% Triton-X100, and then incubated in Block Ace solution (DS Pharma Biomedical, Osaka, Japan). HPPL cultured in 3D conditions were treated as reported previously (Tanimizu *et al.*, 2007). Primary antibodies used for immunofluorescence were mouse anti–β-catenin (1:1500; BS Biosciences), rabbit anti-Cldn3 (1:500; Bioworld, Minneapolis, MN), rabbit anti-Cldn4 (1:500; a gift from Mikio Furuse, Kobe University, Kobe, Japan), rat anti-ZO1 (1:2000; a gift from Bruce Stevenson, University of Alberta, Edmonton, Canada), rat anti-EpCAM (1:500; BD Biosciences), rabbit anti-laminin (1:1000; Sigma-Aldrich, St. Louis, MO), and rabbit anti-Grhl2 (1:350; Sigma-Aldrich). Signals were visualized with Alexa Fluor–conjugated secondary antibodies (Molecular Probes, Eugene, OR) used at a dilution of 1:500. F-Actin bundles were detected with Alexa Fluor 488– or 633–conjugated phalloidin (Molecular Probes) at a dilution of 1:250. Nuclei were counterstained with Hoechst 34580. Samples were examined on Zeiss LSM 510 (Zeiss, Jena, Germany) and Olympus FV1000D IX81 (Olympus, Tokyo, Japan) confocal laser scanning fluorescence microscopes.

Live cell imaging

HPPL expressing yellow fluorescent protein–actin were kept in 5% Matrigel for 2.5 d in a two-well coverglass chamber (Nunc/Thermo Fisher Scientific, Rochester, NY) and then set onto the stage of an Olympus ID51 FV1000. The temperature and CO_2 concentration were kept at 37°C and 5%, respectively. Fifteen points were selected and followed for 32 h. Every 40 min, an *xy* image was captured at each point.

Measurement of transepithelial resistance and paracellular tracer flux

Aliquots of 2×10^5 cells were plated on a 12-mm Transwell with 0.4-μm-pore polyester membrane (Corning, Corning, NY). Transepithelial resistance (TER) was measured directly in culture medium using a Millicell-ERS epithelial volt-ohm meter (Millipore, Billerica, MA) at day 3 of the culture. The TER values were calculated by subtracting the background TER of blank filters, followed by multiplying by the surface area of the filter (1.12 cm^2). For the paracellular tracer flux assay, 4-kDa FITC-dextran (Sigma-Aldrich) was added to the medium inside the Transwell at day 3 at a concentration of 1 mg/ml. After incubation for 2 h, an aliquot of medium was collected from the basal compartment. The paracellular tracer flux was determined as the amount of FITC-dextran in the basal medium, which was measured with an Arvo SX fluorometer (PerkinElmer, Waltham, MA).

SDS–PAGE and immunoblotting

HPPL were cultured on a 12-mm Transwell, washed three times with ice-cold PBS, and then lysed in 150 μl of PBS containing 1% Triton-X as previously reported (Yoshii *et al.*, 2005). After scraping of cells into a microcentrifuge tube, they were placed on ice with several agitations, followed by centrifugation at 20,400 × *g* for 30 min. The supernatant was used as the Triton-X–soluble fraction. The pellet was added with 150 μl of PBS containing 0.1% SDS and then treated with an ultrasonicator. After centrifugation, the supernatant was transferred into a new tube and used as the Triton-X–insoluble fraction. Samples were separated by one-dimensional SDS–PAGE. For immunoblotting, proteins were electrophoretically transferred from gels onto Immobilon-P, a polyvinylidene difluoride membrane (Millipore). After incubation in Block Ace, the membrane was incubated with primary antibodies, including anti-Cldn2, 4, 6, and 8 (1:1000; gifts from Mikio Furuse), anti-Cldn3 (1:1000; Bioworld), anti-Cldn7 (1:1000; Abcam, Cambridge, MA), rabbit anti–cytokeratin 19 (CK19; 1:2000; Tanimizu *et al.*,

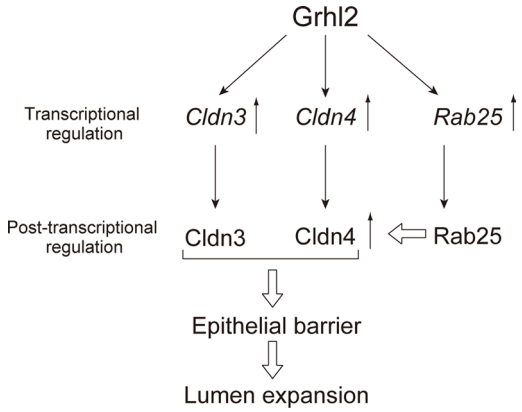

FIGURE 8: A molecular network governed by Grhl2 regulates the lumen size by modulating epithelial barrier function. Our results indicate that Grhl2 transcriptionally regulates Cldn3 and Cldn4, as well as Rab25, for enhancing epithelial morphogenesis, in particular, increasing the size of lumen. Cldns contribute to enhancing the barrier function of the HPPL monolayer, which is essential for the expansion of a central lumen of the cyst in 3D culture. Rab25 up-regulates Cldn4 protein and also promotes its localization at TJs, which induces lumen expansion.

2003), anti–glyceraldehyde-3-phosphate dehydrogenase (1:1000; Millipore). Bound antibodies were detected with horseradish peroxidase–conjugated secondary antibodies. SuperSignal West Dura Extended Duration Substrate (Pierce, Thermo Fisher Scientific, Rockford, IL) was used for the detection of peroxidase activity.

Culture with GST–C-CPE

pGEX6P-1 vector containing C-CPE and C-CPE313 were kindly provided by Mikio Furuse. GST proteins were purified using a glutathione–Sepharose 4B column (Amersham Pharmacia Biotech, Little Chalfont, United Kingdom) as previously reported. Eluted GST fusion proteins were dialyzed against PBS by using Amicon Ultracel-10K (Millipore). HPPL-Grhl2 were plated on the mixture of Matrigel and type I collagen (1:1, vol/vol) and covered with 5% Matrigel containing 100 μg/ml GST-C-CPE or GST-C-CPE313. Cells were kept at 37°C for 7 d.

Statistical analysis

The diameter of lumen was measured for >50 cysts in each culture. Culture was repeated at least three times. We confirmed that all the cultures for each set of HPPL transfectants gave similar results, and then we used a representative culture for each set of transfectants to show a dot plot in the figures. A *t* test was performed on Excel (Microsoft, Redmond, WA) to examine whether the diameter of a lumen was changed by expression of a gene of interest or by addition of peptides with statistical significance.

ACKNOWLEDGMENTS

We thank Mikio Furuse for providing us with antibodies against claudins and plasmid for expression of CPE peptides and for helpful discussions. We also thank Osamu Obara for providing us with cDNA of Grhl2. We appreciate the valuable technical assistance of Shigeru Saito and Eiko Saijo. We thank the members of the Miyajima and Mitaka laboratories for helpful discussions. This work was supported by a pilot grant from the University of California, San Francisco, Liver Center to N.T., National Institutes of Health Grants R01DK083330 and R01AI25144 to K.M., and research grants from the Ministry of Education, Culture, Sports, Science, and Technology, Japan, to N.T., A.M., and T.M.

REFERENCES

Antoniou A, Raynaud P, Cordi S, Zong Y, Tronche F, Stanger BZ, Jacquemin P, Pierreux CE, Clotman F, Lemaigre FP (2009). Intrahepatic bile ducts develop according to a new mode of tubulogenesis regulated by the transcription factor SOX9. Gastroenterology 136, 2325–2333.

Bagnat M, Cheung ID, Mostov KE, Stainier DY (2007). Genetic control of single lumen formation in the zebrafish gut. Nat Cell Biol 9, 954–960.

Bryant DM, Datta A, Rodriguez-Fraticelli AE, Peranen J, Martin-Belmonte F, Mostov KE (2010). A molecular network for de novo generation of the apical surface and lumen. Nat Cell Biol 12, 1035–1045.

Bryant DM, Mostov KE (2008). From cells to organs: building polarized tissue. Nat Rev Mol Cell Biol 9, 887–901.

Casanova JE, Wang X, Kumar R, Bhartur SG, Navarre J, Woodrum JE, Altschuler Y, Ray GS, Goldenring JR (1999). Association of Rab25 and Rab11a with the apical recycling system of polarized Madin-Darby canine kidney cells. Mol Biol Cell 10, 47–61.

Cheung ID, Bagnat M, Ma TP, Datta A, Evason K, Moore JC, Lawson ND, Mostov KE, Moens CB, Stainier DY (2011). Regulation of intrahepatic biliary duct morphogenesis by Claudin 15-like b. Dev Biol 361, 68–78.

Fitz JG (2002). Regulation of cholangiocyte secretion. Semin Liver Dis 22, 241–249.

Goldenring JR, Shen KR, Vaughan HD, Modlin IM (1993). Identification of a small GTP-binding protein, Rab25, expressed in the gastrointestinal mucosa, kidney, and lung. J Biol Chem 268, 18419–18422.

Gray RS, Cheung KJ, Ewald AJ (2010). Cellular mechanisms regulating epithelial morphogenesis and cancer invasion. Curr Opin Cell Biol 22, 640–650.

Lemaigre FP (2003). Development of the biliary tract. Mech Dev 120, 81–87.

Martin-Belmonte F, Mostov K (2008). Regulation of cell polarity during epithelial morphogenesis. Curr Opin Cell Biol 20, 227–234.

Moriwaki K, Tsukita S, Furuse M (2007). Tight junctions containing claudin 4 and 6 are essential for blastocyst formation in preimplantation mouse embryos. Dev Biol 312, 509–522.

Nam KT *et al.* (2010). Loss of Rab25 promotes the development of intestinal neoplasia in mice and is associated with human colorectal adenocarcinomas. J Clin Invest 120, 840–849.

Okabe M, Tsukahara Y, Tanaka M, Suzuki K, Saito S, Kamiya Y, Tsujimura T, Nakamura K, Miyajima A (2009). Potential hepatic stem cells reside in EpCAM+ cells of normal and injured mouse liver. Development 136, 1951–1960.

Pyrgaki C, Liu A, Niswander L (2011). Grainyhead-like 2 regulates neural tube closure and adhesion molecule expression during neural fold fusion. Dev Biol 353, 38–49.

Tanimizu N, Miyajima A, Mostov KE (2007). Liver progenitor cells develop cholangiocyte-type epithelial polarity in three-dimensional culture. Mol Biol Cell 18, 1472–1479.

Tanimizu N, Nishikawa M, Saito H, Tsujimura T, Miyajima A (2003). Isolation of hepatoblasts based on the expression of Dlk/Pref-1. J Cell Sci 116, 1775–1786.

Tsukita S, Furuse M (2002). Claudin-based barrier in simple and stratified cellular sheets. Curr Opin Cell Biol 14, 531–536.

Tzaban S, Massol RH, Yen E, Hamman W, Frank SR, Lapierre LA, Hansen SH, Goldenring JR, Blumberg RS, Lencer WI (2009). The recycling and transcytotic pathways for IgG transport by FcRn are distinct and display an inherent polarity. J Cell Biol 185, 673–684.

Werth M *et al.* (2010). The transcription factor grainyhead-like 2 regulates the molecular composition of the epithelial apical junctional complex. Development 137, 3835–3845.

Wilanowski T *et al.* (2008). Perturbed desmosomal cadherin expression in grainy head-like 1-null mice. EMBO J 27, 886–897.

Yoshii T, Mizuno K, Hirose T, Nakajima A, Sekihara H, Ohno S (2005). sPAR-3, a splicing variant of PAR-3, shows cellular localization and an expression pattern different from that of PAR-3 during enterocyte polarization. Am J Physiol Gastrointest Liver Physiol 288, G564–G570.

Yu Z, Bhandari A, Mannik J, Pham T, Xu X, Andersen B (2008). Grainyhead-like factor Get1/Grhl3 regulates formation of the epidermal leading edge during eyelid closure. Dev Biol 319, 56–67.

Yu Z, Mannik J, Soto A, Lin KK, Andersen B (2009). The epidermal differentiation-associated Grainyhead gene Get1/Grhl3 also regulates urothelial differentiation. EMBO J 28, 1890–1903.

Zegers MM, O'Brien LE, Yu W, Datta A, Mostov KE (2003). Epithelial polarity and tubulogenesis in vitro. Trends Cell Biol 13, 169–176.

Zong Y, Panikkar A, Xu J, Antoniou A, Raynaud P, Lemaigre F, Stanger BZ (2009). Notch signaling controls liver development by regulating biliary differentiation. Development 136, 1727–1739.